# High carrier suppression double sideband modulation with integrated LiNbO$_3$ optical modulators  for photonic local oscillators (An alternative scheme of Laser Synthesizer)

**Tetsuya Kawanishi[1], Hitoshi Kiuchi[2], Masumi Yamada[2], Takahide Sakamoto[1], Masahiro Tsuchiya[1], Jun Amagai[1], and Masayuki Izutsu[1]**

1 National Institute of Information and Communications Technology, 4-2-1 Nukui-Kita, Koganei, Tokyo, 184-8795, Japan

2 National Astronomical Observatory of Japan, 2-21-1 Osawa, Mitaka, Tokyo 181-8588, Japan

*Abstract* —**We proposed high carrier suppression double sideband modulation using a Mach-Zehnder (MZ) optical modulator with active trimming technique. The modulator has a pair of trimmers in the arms of the MZ structure. The trimmers can compensate amplitude imbalance in the MZ structure due to fabrication error, where the imbalance generates residual carrier in double sideband suppressed carrier (DSB-SC) modulation. We demonstrated high carrier suppression ratio of 50dB in DSB-SC modulation at 10.5GHz, by using an integrated MZ LiNbO$_3$ modulator, where each arm has an intensity trimmer consisting of a sub MZ interferometer. In addition, we also proposed a novel scheme for the fourth order harmonic generation with two MZ modulators. A photonic local signal of 42GHz was generated from a 10.5GHz modulating signal. The upper limit of modulating frequency in the state-of-the-art is about 50GHz, so that we can easily generate 200GHz photonic local signals by using this technique.**

*Index Terms* — **Double sideband suppressed carrier, optical modulation, Mach-Zehnder structure, amplitude imbalance, active trimmer, high carrier suppression**

## I. INTRODUCTION

  Radio-on-fibre technique has been investigated for various micro/millimetre-wave systems, such as pico-cellular mobile networks [1], photonic local-oscillators (LOs) for millimetre-wave radio astronomy [2], etc. Two-tone lightwave signal generation techniques are useful for micro/millimetre-wave fibre links, because undesired dispersion effect in a fibre can be suppressed and the rf-signal frequency at receiver side is double the modulation frequency at transmitter side [3]. In addition, the conversion efficiency from lightwave to micro/millimetre wave is larger than in amplitude modulation with carrier. A mode-locked laser or phase-locked two laser sources can generate two-tone signals for photonic LOs. However, the phase lock condition of the two-tone signal should be stably maintained in order to obtain low noise micro/millimetre signals. Optical phase difference between the spectrum components in the two-tone signal is very sensitive to mechanical vibration, temperature change, electric noise, etc. Another technique for two-tone signal generation is double-sideband suppressed carrier (DSB-SC) optical modulation, where the optical frequency difference between the spectrum components is precisely equal to the frequency of the modulating signal. The merit of this technique is stable phase relations in the two-tone signal. The spectrum components generated by optical modulation are always phase-locked, so that we can easily construct robust photonic LO systems without using complicated feedback control techniques.

  LiNbO$_3$ Mach-Zehnder (MZ) optical intensity modulators have been widely used for optical DSB-SC modulation. However, the carrier suppression ratio is dominated by the on-off extinction ratio of the MZ modulator. A typical extinction ratio of a MZ modulator is less than 35dB. The extinction ratio depends on the MZ waveguide structure and is limited by fabrication errors in the waveguide structures. Crosstalk between the fundamental waveguide mode and high-order radiative modes also degrades the extinction ratio. For advanced fibre links such as photonic LO distribution systems for sub THz radio astronomy measurement, the carrier suppression ratio should be larger than in conventional techniques. In this paper, we propose a novel high extinction ratio optical intensity modulation technique for DSB-SC modulation. Imbalance in the MZ structure can be compensated by trimmers in MZ arms. Generation of DSB-SC lightwave signal with high carrier suppuration ratio was demonstrated by using the MZ modulator with trimmers, where the on-off extinction ratio was 50dB. Micro/millimetre-waves of 21GHz and 40GHz were generated from 10.5Hz and 20GHz modulating signals, respectively. We also proposed the fourth order harmonic generation technique using two MZ modulators which are connected in series. A 42GHz millimetre-wave signal was generated from 10.5GHz modulating signals, by using this technique. The upper limit of modulating frequency in the state-of-the-art is about 50GHz, so that we can obtain high-frequency photonic LO signals up to 200GHz, with stable phase-locking.

## II. MACH-ZEHNDER OPTICAL MODULATOR WITH INTENSITY TRIMMERS

  Figure 1 (a) shows the principle of the MZ modulator, which has two arms and an electrode. The optical phase in each arm can be controlled by changing the voltage applied on the electrode. When the lightwaves are in phase, the modulator is in

"on" state. On the other hand, when the lightwaves are in opposite phase, the lightwave is converted into a high-order radiative mode wave which can not propagate the waveguide for output.
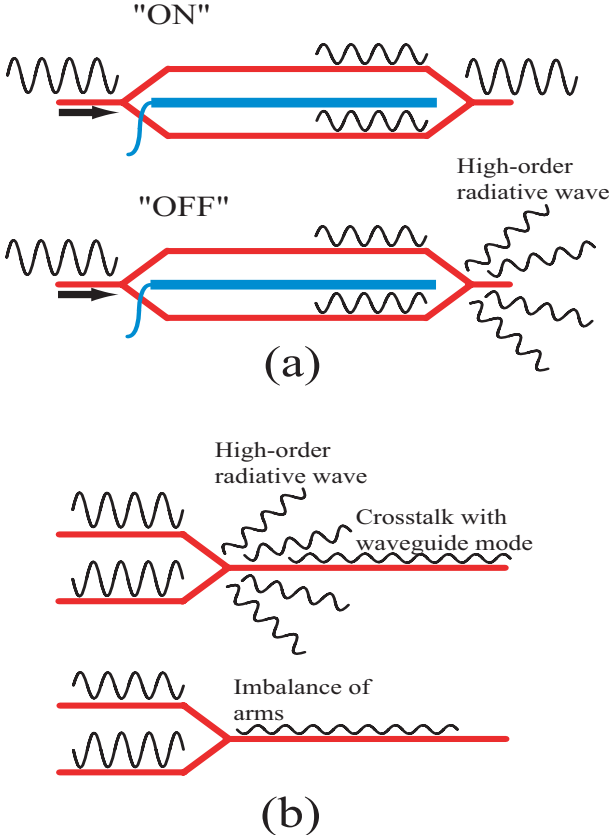


Fig. 1 (a) Principle of Optical intensity modulation by an MZ modulator. (b) Residual optical output when the modulator is off.



Fig. 2 MZ modulator with intensity trimmers.

Thus, we turn the modulator "on" and "off" by changing the voltage on the electrode. However, there is some residual lightwave even in the "off" state, due to amplitude imbalance in the arms, and crosstalk between the high-order and waveguide modes as shown in figure 1 (b). In this paper, we focus on the imbalance of the arms. Figure 2 shows an MZ modulator having two intensity trimmers in the arms. By using the trimmers, we can compensate the amplitude imbalance due to fabrication errors, where the intensity trimmers can be also constructed by MZ structures.

## III. DOUBLE-SIDEBAND SUPPRESSED CARRIER MODULATION FOR THE SECOND ORDER HARMONIC GENERATION

To demonstrate the compensation of the fabrication error, we used an integrated optical modulator which has a pair of MZ structures in a main MZ structure, as shown in figure 3. The modulator has three electrodes (A, B and C). We can actively control the amplitude balance between the arms, by changing dc-bias voltages on the electrodes A and B. A modulation signal should be fed to the electrode C which changes the optical phase difference between the arms of the main MZ structure. The half-wave voltage of the electrodes A and B was 4.2V, while that of the electrode C was 6.1V.
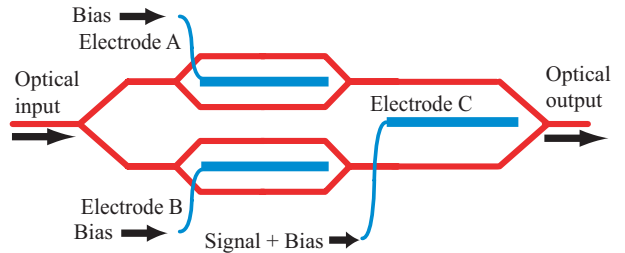


Fig. 3 High extinction intensity modulation using an integrated optical modulator consisting of two MZ structures.

We can maximize the extinction ratio of the intensity modulation, by the following steps: 1) adjusting the bias voltages on A, B and C (bias A, B and C, henceforth) to maximize the output optical power, 2) adjusting the bias C to minimize the output power, 3) stirring the bias A or B, where slight change of one (bias A or B) causes reduction of the output power, but the other increases it, 4) minimization of the output by using the bias which decreases the power in the previous step, and the bias C. In the last step, we can obtain optimal bias voltages A and B for high extinction ratio intensity modulation. The bias C should be a quadrature point which corresponds to an average of the bias C voltages in the steps 1) and 4). Figure 4 shows measured responses of the modulator to the bias C with and without the imbalance compensation technique described above, where the x-axis is normalized by the half-wave voltage of the electrode C and the zero corresponds to the "off" state. We also measured the response without the compensation technique after the step 1), as shown in figure 5. The input power and wavelength were 2.7dBm and 1550nm, respectively. The maximum optical powers with and without compensation were, respectively, -0.7dBm and -0.4dBm. The extinction ratios with and without compensation were, respectively, 50.3dB and 37.5dB.

In our experiment, we used the bias A in the step 4). It means that the optical intensity in the upper arm of the fabricated main MZ is larger than in the lower arm when the compensation technique is not used. Figure 6 shows optical response on the bias A, where the x-axis is normalized by the half-wave voltage of the electrode A and the zero equals the voltage of the step 1) which gives the maximum optical output. The bias C is fixed at the voltage of the step 4). The normalized bias

voltage on the electrode A for the compensation was 0.143, which corresponds to 2.5% amplitude reduction in the upper arm. Thus, residual output in the "off" state without compensation should be -32dB (= 20 log 0.025), where the measured result was -37.5dB. We deduce that the difference is caused by interference between the residual components due to the crosstalk and to the imbalance shown in figure 1 (b), in addition to the errors in our measurement.
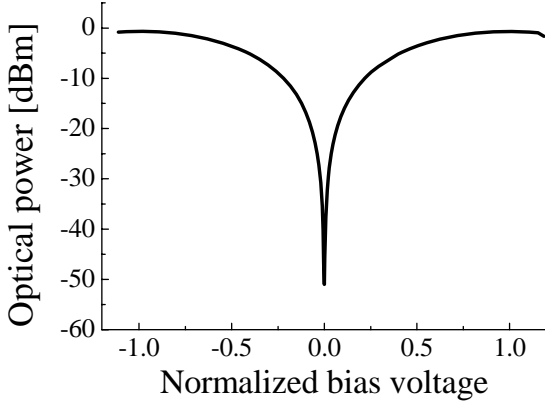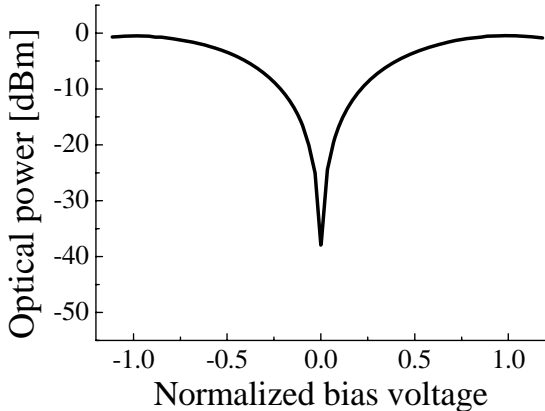


Fig. 4 Optical response to bias C with imbalance compensation.



Fig. 5 Optical response to bias C without imbalance compensation.
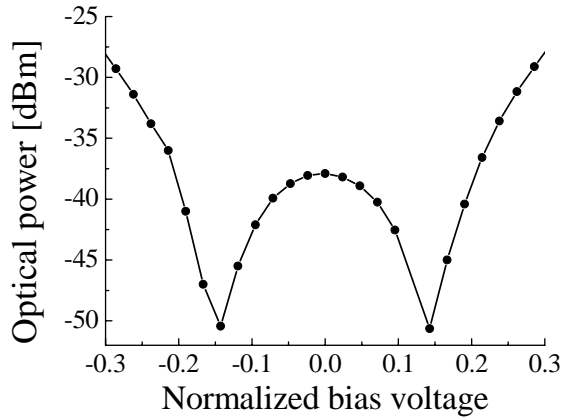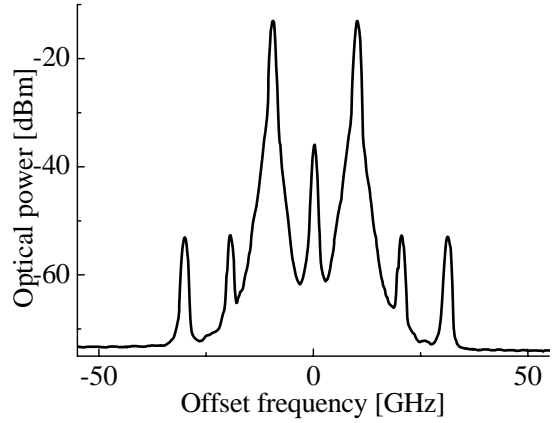


Fig. 6 Optical response to bias A.



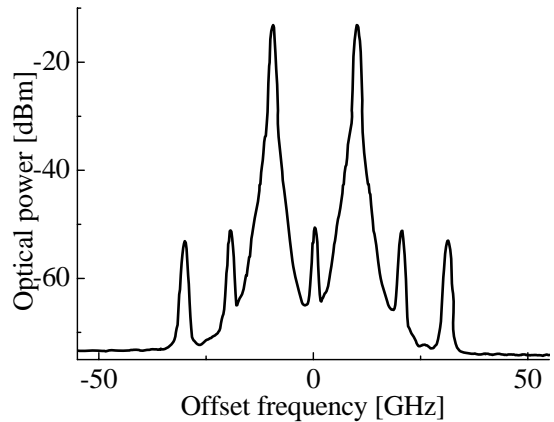Fig. 7 Optical spectrum of DSB-SC signal without trimming technique.



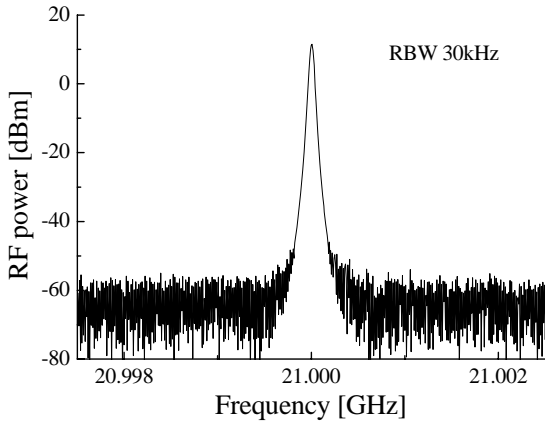Fig. 8 Optical spectrum of DSB-SC signal with trimming technique.

3

*Fig. 9 RF spectrum of microwave generated from DSB-SC signal. Modulating frequency was 10.5GHz.*
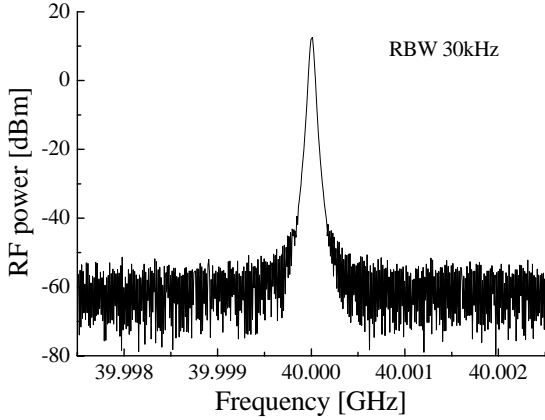


*Fig. 10 RF spectrum of microwave generated from DSB-SC signal. Modulating frequency was 20GHz.*
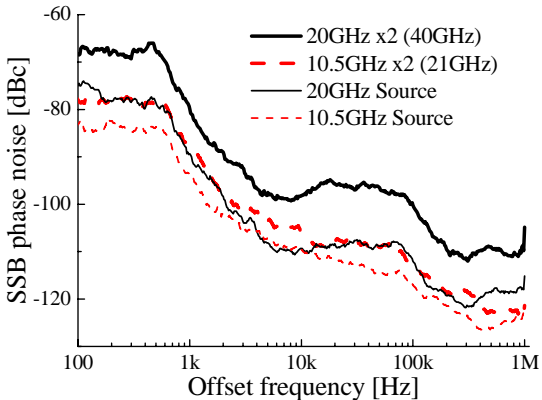


*Fig. 11 SSB phase noises of generated millimetre/micro-wave signals and source microwaves.*

By using the trimming technique mentioned above, we dem-

onstrated DSB-SC modulation to generate a dual-mode lightwave signal. We applied a sinusoidal microwave signal to the electrode C. The modulating frequency $f_m$ was 10.5GHz, the rf power at the electrode C was 19dBm. The bias C was set to be in a null point. Figure 7 shows the optical spectrum of a DSB-SC signal without using the trimming technique, where the carrier suppression ratio with respect to the first order components was 22.9dB. As shown in figure 8, the carrier was successfully suppressed by using the active trimming technique. The suppression ratio was 37.5dB. The optical power of desired components (the sum of the first order sideband components) was -10.2dBm. The second order harmonic generation was mainly due to residual optical phase modulation in the MZ modulator caused by imbalance in optical modulation efficiency between the arms. The third order components are due to intrinsic nonlinearity of the MZ structure. By feeding the optical signal to a high-speed photodetector, we demonstrated generation of a microwave signal whose frequency should be double the modulating frequency $f_m$. Figure 9 shows the rf spectrum of the generated microwave whose frequency was 21GHz. The output was quite stable, and the line width was less than 1Hz. We also demonstrated generation of a millimetre wave at 40GHz by using the DSB-SC modulation with the active trimming technique, as shown in figure 10. SSB phase noise plots of the micro/millimetre-waves were also measured as described in figure 11, where phase noises for source sinusoidal microwave signals ($f_m$=10.5GHz and 20GHz) fed to the electrode C were also measured for comparison. The phase noise of 21GHz signal generated by DSB-SC modulation was almost equal to that of the 20GHz source signal. Thus, we deduce that phase noise due to the DSB-SC modulation scheme was small enough with respect to the noise from the measurement setup. The phase noises of $f_m$=10.5 GHz and 21GHz were, respectively, -98.2 dBc/Hz and -106.0 dBc/Hz at 10 kHz offset.

This conventional phase noise measurement involved a reference signal phase noise. On the other hand, by using a DMTD (Dual-Mixer Time Difference) method, we can measure the system instability as an Allan variance free from the reference phase noise and calculate the coherence loss from the measured phase stability.

Noises can be classified into five types according to the noise generation mechanism..

White PM (phase modulation) noise ($\tau^{-1}$) is caused by the additive noise that always overlaps signals generated with the oscillator. Thermal noise is an example of the additive noise in the low frequency region of electro-magnetic wave.

Flicker PM noise ($\tau^{-1}$) is produced by phase modulation of flicker noise caused by the non-linearity of circuit devices.

White FM (frequency modulation) noise ($\tau^{-1/2}$) is produced by disturbed oscillation caused by the noise in the oscillator loop within the oscillator. Its amplitude depends on the oscillator Q value, which represents the sharpness of oscillation.

Flicker FM noise ($\tau^0$) and Random walk noise ($\tau^{+1/2}$) are the factors limiting the long-term stability. These types of noises are also produced in electronic circuits and frequency standards, depending on the environmental conditions.

The frequency stability of the reference signal for the short-time periods is an important factor in maintaining the coherence of received signals in interferometer experiments. The fractional loss of coherence due to the instability in the frequency standard for **T-sec** integration times is estimated by Eq. (1)[4].

$$L_c = \omega_o^2 \ [\alpha_p/6 + \alpha_f/12*T + \sigma_y^2/57*T^2] \qquad (1)$$

where

$L_c$    the loss of coherence,
$\omega_o$    the angular frequency of local oscillator,
$\alpha_p$    the Allan variance of white phase noise at l sec,
$\alpha_f$    the Allan variance of white frequency noise at l sec,
$\sigma_y^2$    the constant Allan variance of flicker frequency noise,
$T$      the integration time [sec].

The DMTD enables time measurements as well as frequency and frequency stability measurements for sample times as short as a few milliseconds or longer, all without dead time. This method is contrived to cancel out the phase noise in the measurement system.

Experimental setup for phase noise measurement is shown in Fig. 12. This is 22 GHz signal configuration. The origin of the source signal is 11 GHz synthesizer, the 11 GHz signal is used for MZ-LN modulation signal and a 22 GHz (spurious of 11GHz) is used for a refer signal (Signal A). Pretty much by definition, 11 GHz and 22 GHz signals are coherence. After optical modulation by the MZ-LN, a two-tone optical signal in 22 GHz difference is generated. A photo-detector converts the two-tone optical signal to a 22 GHz microwave signal (Signal B). Both 22 GHz signals (Signal A and B) are frequency converted to 20 MHz by a common 21.98 GHz signal. Finally, phase differential between the 20 MHz signals are measured by a DMTD. In this case, the 21.98 GHz synthesizer, the hybrid, and mixers in Fig. 12 compose a kind of DMTD. During these operations, the 20 MHz signals are free from instabilities of the 11 GHz and 21.98 GHz synthesizers. The measured phase stability on Allan variance is shown in Fig. 13.
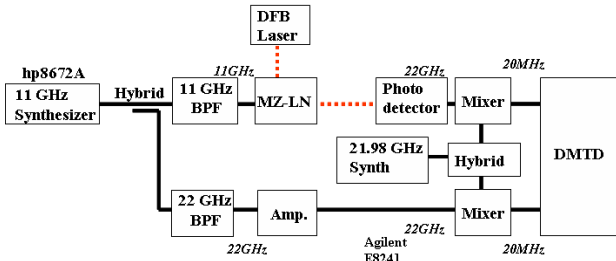


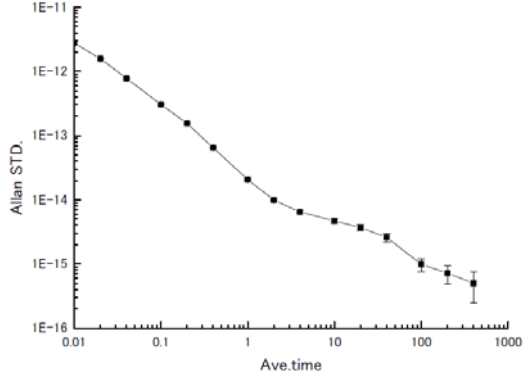*Fig. 12 Experimental setup for phase stability measurement.*



*Fig. 13 Phase stability in Allan variance.*

The key of an interferometer is to maintain the signal coherence. In a connected interferometer, the instability of the frequency distributed by the common reference in central element is compensated for as a common noise. On the other hand, the reference signal phase noise can not be dealt with common noise for cross correlation between sub-arrays and VLBI experiments. Therefore the Laser Synthesizer (LS) is required to maintain the signal coherence. The estimated coherence loss of the MZ-LN modulator system is 0.25 %,or 3.1 % given the embossment at 30-second is caused by the white FM.. This shows that the LN modulator is applicable to VLBI experiments as an alternative scheme of LS.

## IV. QUADPLEX DOUBLE-SIDEBAND SUPPRESSED CARRIER MODULATION FOR THE FOURTH ORDER HARMONIC GENERATION

The optical modulation frequency is limited by the loss at the electrode in the MZ modulators. Thus, the frequency of the photonic LO signal generated by DSB-SC modulation described in the previous section would be lower than 100GHz. In this section, we propose a novel technique which can generate the fourth order harmonic components with high carrier suppression ratio, in order to obtain high-frequency photonic LO signals up to 200GHz. The second order upper and lower sideband (USB and LSB) components can be obtained by using two MZ modulators which are connected in series, as shown in figure 14. The first order USB and LSB components are generated at the first MZ modulator, where the carrier component is highly suppressed. The optical frequency of the USB is $f_0+f_m$, and that of the LSB is $f_0-f_m$, where $f_0$ is the optical frequency of the lightwave from the laser source in figure 14. In this paper, a spectral component whose frequency is $f_0+Nf_m$ is henceforth called $f_0+Nf_m$ component. At the second modulator, the $f_0+f_m$ component (the USB at the first modulator) is converted into $f_0$ and $f_0+2f_m$ components. At the same time, $f_0$ and $f_0-2f_m$ components are generated from the $f_0-f_m$ component (the LSB at the first modulator). Thus, there are three spectrum components: $f_0$, $f_0+2f_m$ and $f_0-2f_m$ in the output of the second modulator. However, we can control the intensity of the $f_0$ component by changing the phase difference between the modulating signal at the first and the second modulator. When the phase difference is equal to 90 degrees, the $f_0$ component from the $f_0+f_m$ component and that from the $f_0-f_m$ component are interfere destructively, so that the carrier $f_0$ component can be suppressed at the output. As shown in figure 14, the output has the $f_0+2f_m$ and $f_0-2f_m$ components, where other components are highly suppressed. Thus, we can obtain a millimetre-wave signal whose

frequency is $4f_m$, by feeding the output lightwave signal to a high-speed photodetector. In this paper, we call this technique for the fourth order harmonic component ($4f_m$), *quadplex DSB-SC modulation*.

We demonstrated generation of 42GHz millimetre-wave from 10.5GHz microwave by using the quadplex DSB-SC modulation technique. Figure 15 shows the output lightwave spectra, where the phase difference between the modulating signals at the first and second modulators are 0 and 90 degrees. In the case of 90 degrees phase difference, the carrier component is largely suppressed, while that in the case of 0 degrees phase difference is larger than the $f_0+2f_m$ and $f_0-2f_m$ components. The phase difference can be adjusted by an optical or electrical delay. In our experiment, we used an electrical delay as shown in figure 14, where the carrier suppression ratio with respect to the $f_0+2f_m$ and $f_0-2f_m$ components was 45.8dB. The suppression ratio of the other components was 34dB, where $f_0+3f_m$ and $f_0-3f_m$ components were most significant. The third order components are due to nonlinearity of optical modulation. The input optical power was 12.7dBm. The modulating signal frequency $f_m$ is 10.5GHz, while the signal powers were 20.9dBm at the first modulator and 21.0dBm at the second modulator. Both of the modulators had active trimmers, and the imbalances in the arms were compensated by using the technique described in the previous sections. We used two polarization controllers at the input ports of the modulators. The insertion losses of the polarization controller were 1.1dBm at the first modulator and 0.4dBm at the second modulator. By feeding the optical output to a high-speed photodetector, we generated millimetre-wave signals, whose frequency domain profiles are shown in figures 16 and 17. The rf powers of $f_m$, $2f_m$, $3f_m$ and $4f_m$ in the output of the photodetector were, respectively, -32.8dBm, -30.8dBm, -35.0dBm and +11dBm, so that the spurious suppression ratio with respect to $4f_m$ component was 41.8dB. As shown in figure 16, the line width of the desired $4f_m$ component (42GHz) was less than 1Hz. SSB phase noise plots of the generated millimetre-wave and the modulating source signal (10.5GHz) were shown in figure 11. The phase noise of the $4f_m$ component was -95.8 dBc/Hz at 10 kHz offset. Figure 17 shows the noise figure of the fourth order harmonic generation by the quadplex DSB-SC, which is defined by the SSB phase noise ratio between the source modulating signal and the generated millimetre-wave signal. The theoretical lower limit of the noise figure is 20 log N dB, where N is the harmonic generation order. In our proposed setup, the theoretical limit should be 20 log 4 = 12dB, while a measured result was 18dB. We deduce that a part of this difference in noise figure is due to noise generated in the optical link shown in figure 14, and the difference of the noise floor of our spectrum analyzer at 10GHz and 42GHz.
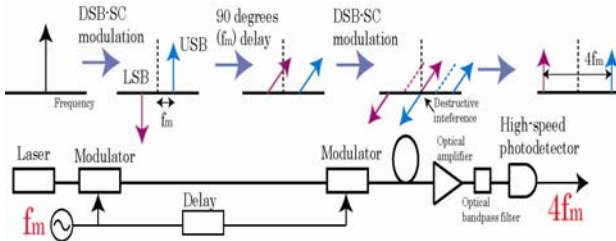


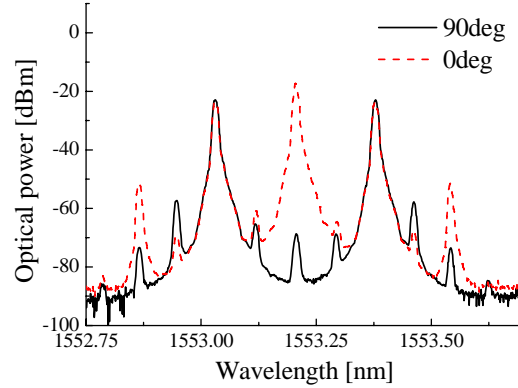*Fig. 14 Principle of quadplex double-sideband suppressed carrier modulation.*



*Fig. 15 Optical spectra of quadplex DSB-SC modulation technique. Solid and dashed lines are for 90 and 0 degrees phase differences.*
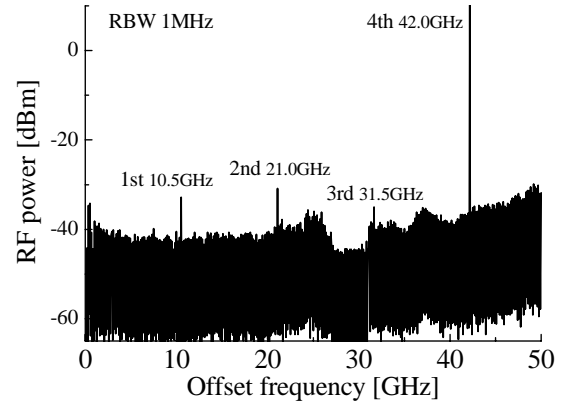


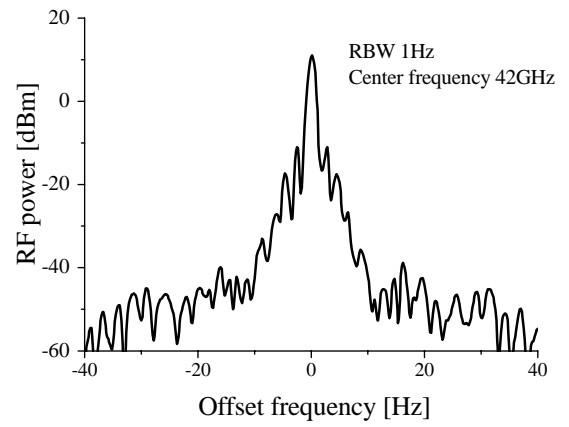*Fig. 16 RF spectrum of quadplex DSB-SC from 0 to 50GHz.*



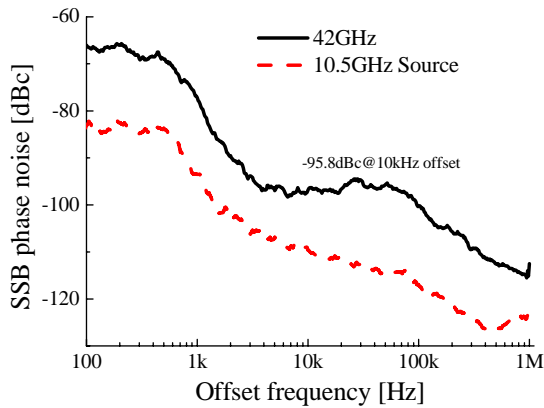*Fig. 16 RF spectrum of quadplex DSB-SC at 42GHz.*

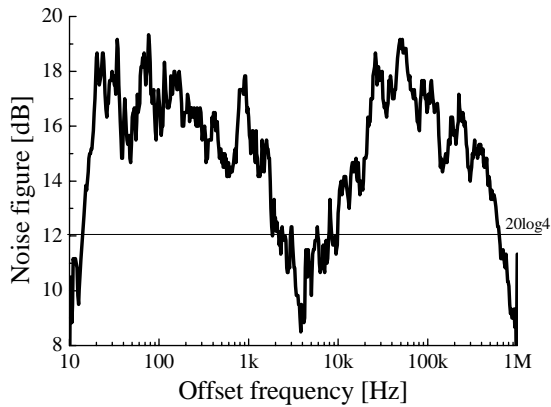*Fig. 17 SSB phase noises of the generated millimetre –wave and the source microwave.*



*Fig. 18 Noise figure between the generated millimetre-wave signal and the source microwave.*

## V. CONCLUSIONS

We proposed a high carrier suppression optical double-sideband intensity modulation technique by using an integrated LiNbO$_3$ MZ modulator, where the imbalance in the MZ arms can be compensated by a pair of active trimmers. The on-off extinction ratio of a fabricated modulator was 50dB. We demonstrated generation of 21GHz and 40GHz rf-signals from 10.5Hz and 20GHz modulating signals by using the modulator. The carrier suppression ratio was 37.5dB, where that of the conventional technique was 22.9 dB. Estimated phase stability and coherence loss are $\sigma_y(1sec)$=1.9E-14 and 0.25 % in turn on 938 GHz local signal. Thus, it is applicable to VLBI experiments. We also proposed a novel modulation technique for the fourth order harmonic generation. A two-tone lightwave whose frequency separation is a quadplex of the modulating frequency can be generated by using two MZ modulators which also have active trimmers for imbalance compensation. A photonic local signal of 42GHz was generated from a 10.5GHz modulating signal, where the spurious suppression ratio was 41.8dB. The

upper limit of modulating frequency in the state-of-the-art is about 50GHz, so that we can easily generate 200GHz photonic local signals by using this technique. The two spectral components in the two-tone signal generated by our technique are stationary phase-locked to each other, without using complicated feedback control. In our measurement, the setup was implemented on a conventional wooden table, where we did not use any temperature or bias control. Temperature change or mechanical vibrations may affect the output lightwave slowly, but there is no chaotic phenomenon, such as mode hopping, mode competition. Thus, we believe that our techniques proposed here should be useful to construct a robust, low-cost and simple setup for photonic LO signals up to 200GHz.

**References**

1 X. Wang et al., IEEE Trans. Microwave Theory and Tech., **48** (2000) 2529
2 A. Ueda et al., Jpn. J. Appl. Phys., **42** (2003) L704
3 J. J. O'Reilly et al., Electron. Lett., **28** (1992) 2309
4 A.E.E.Rogers et al., IEEE Trans. Instrum. Meas., **30** (1981) 283.
5 H. Kiuchi, ALMA memo 530